Figure S1
Click here to download high resolution image

Figure S1

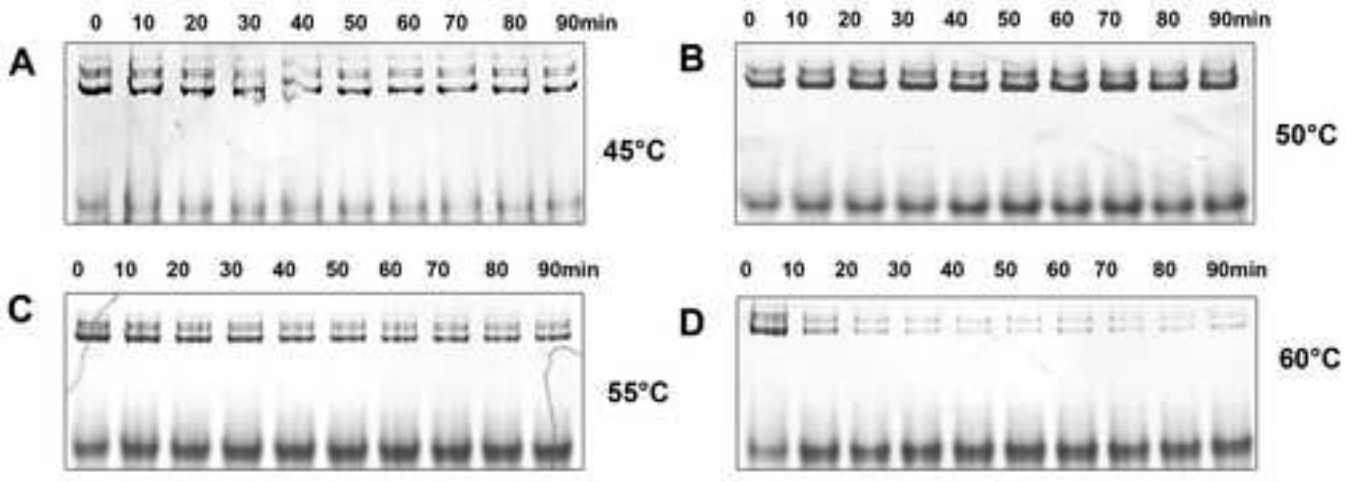

Figure S2
Click here to download high resolution image

Figure S2

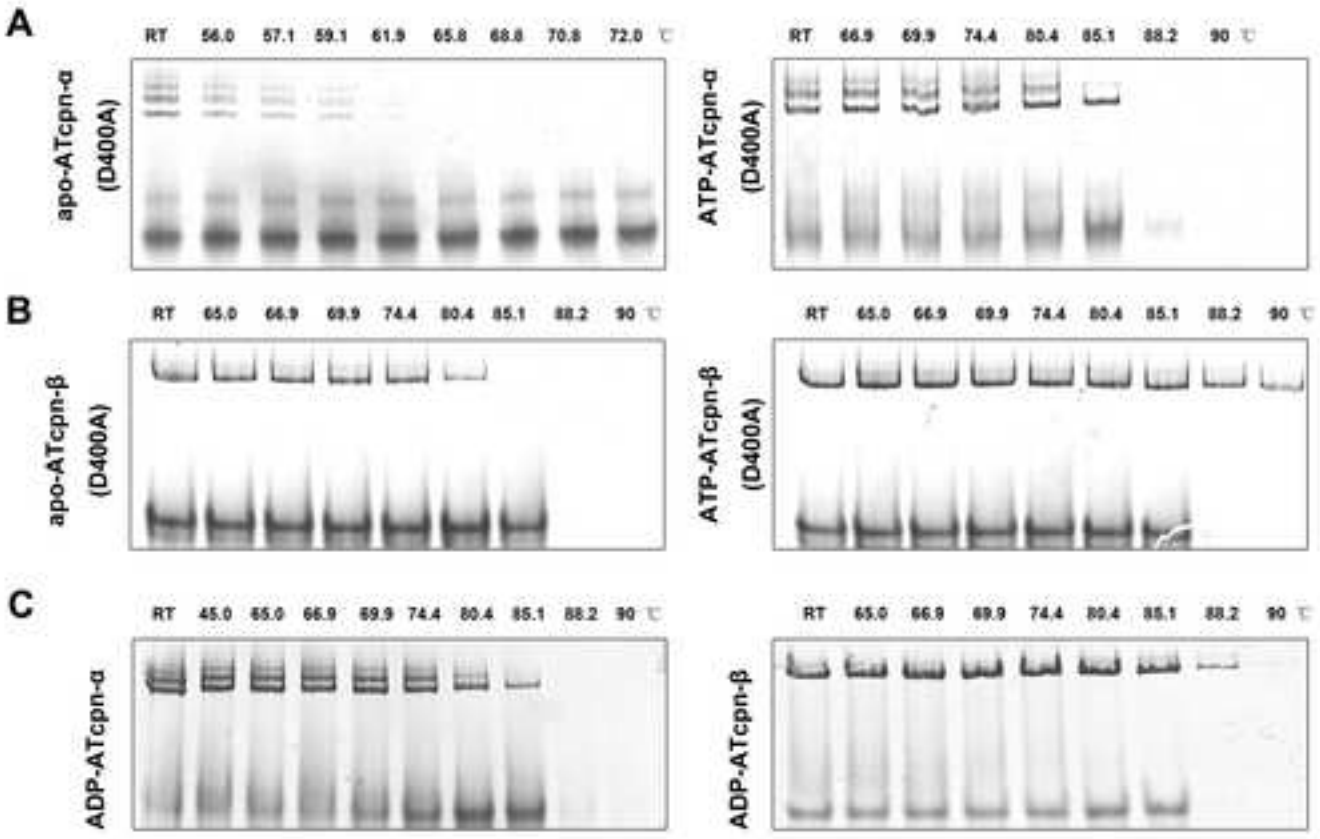

Figure S3
Click here to download high resolution image

Figure S3

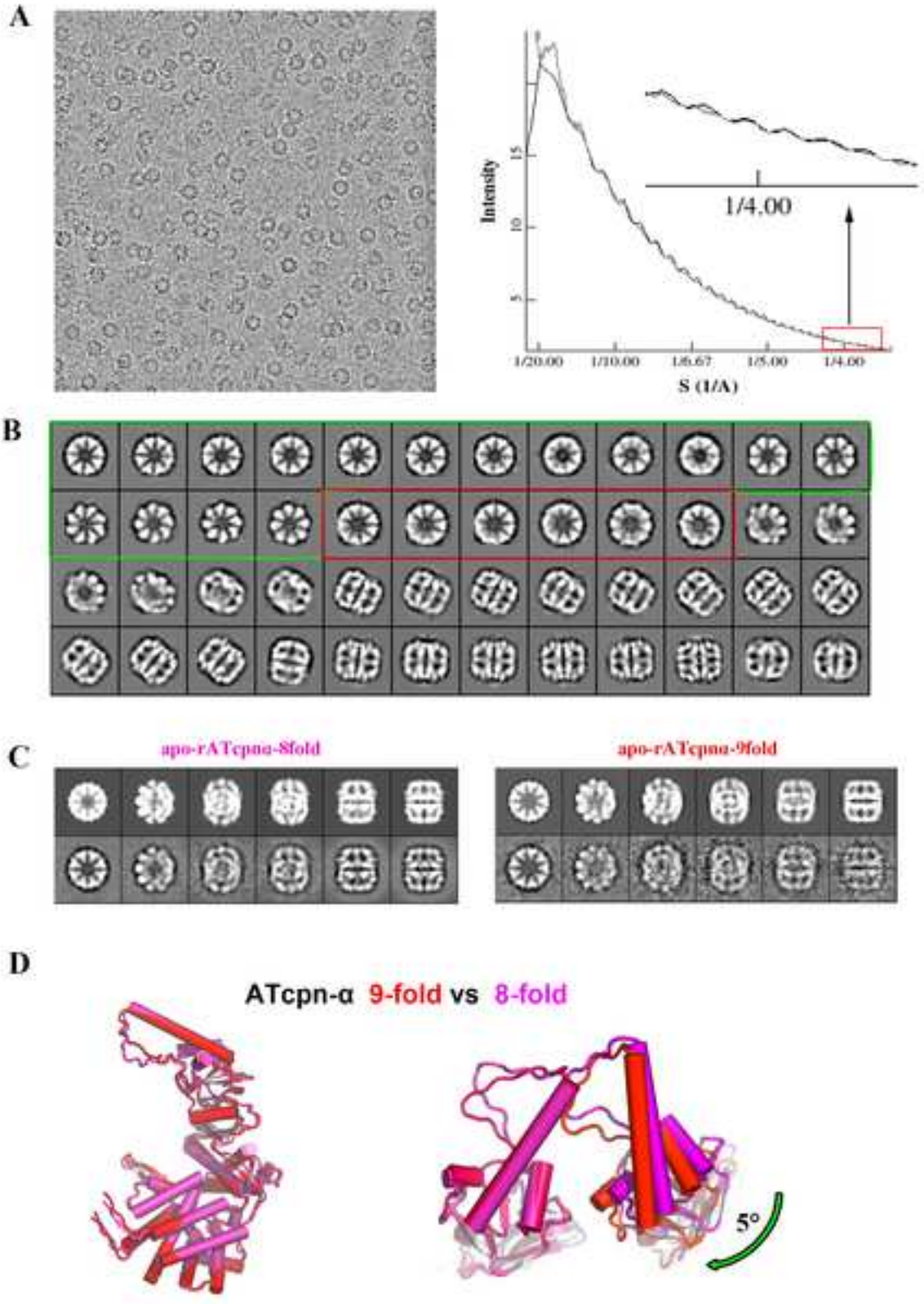

Figure S4
Click here to download high resolution image

Figure S4

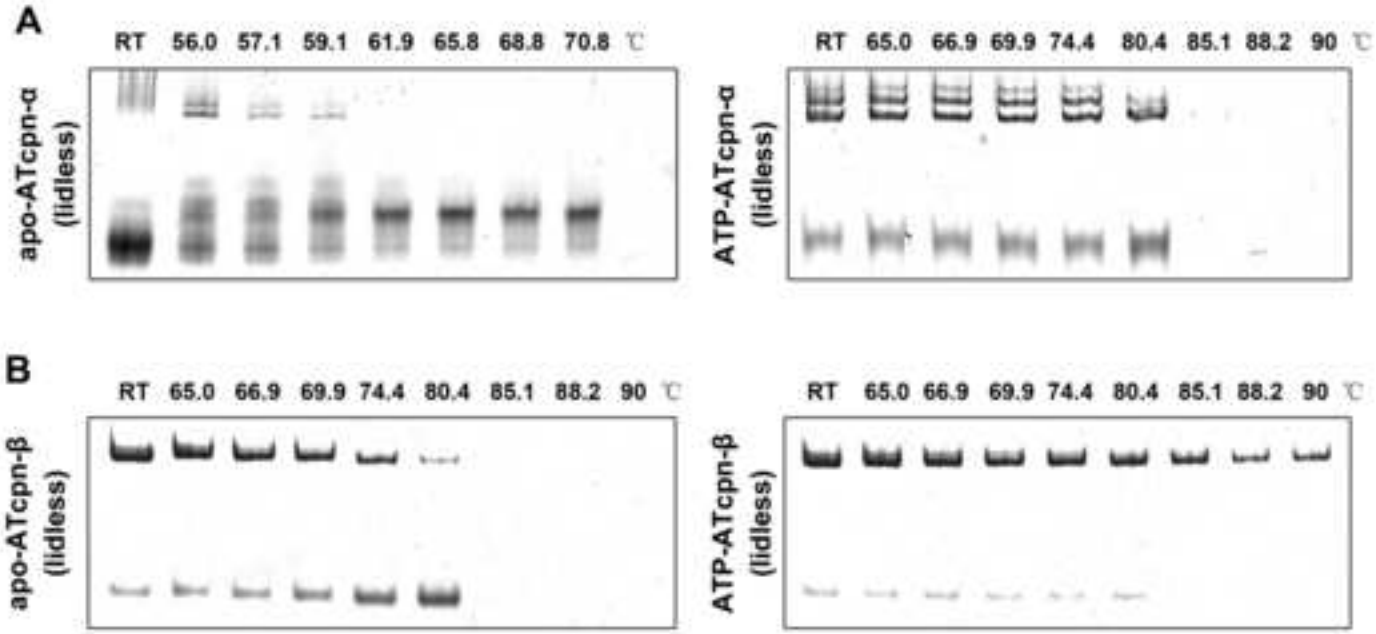

Figure S5
Click here to download high resolution image

Figure S5

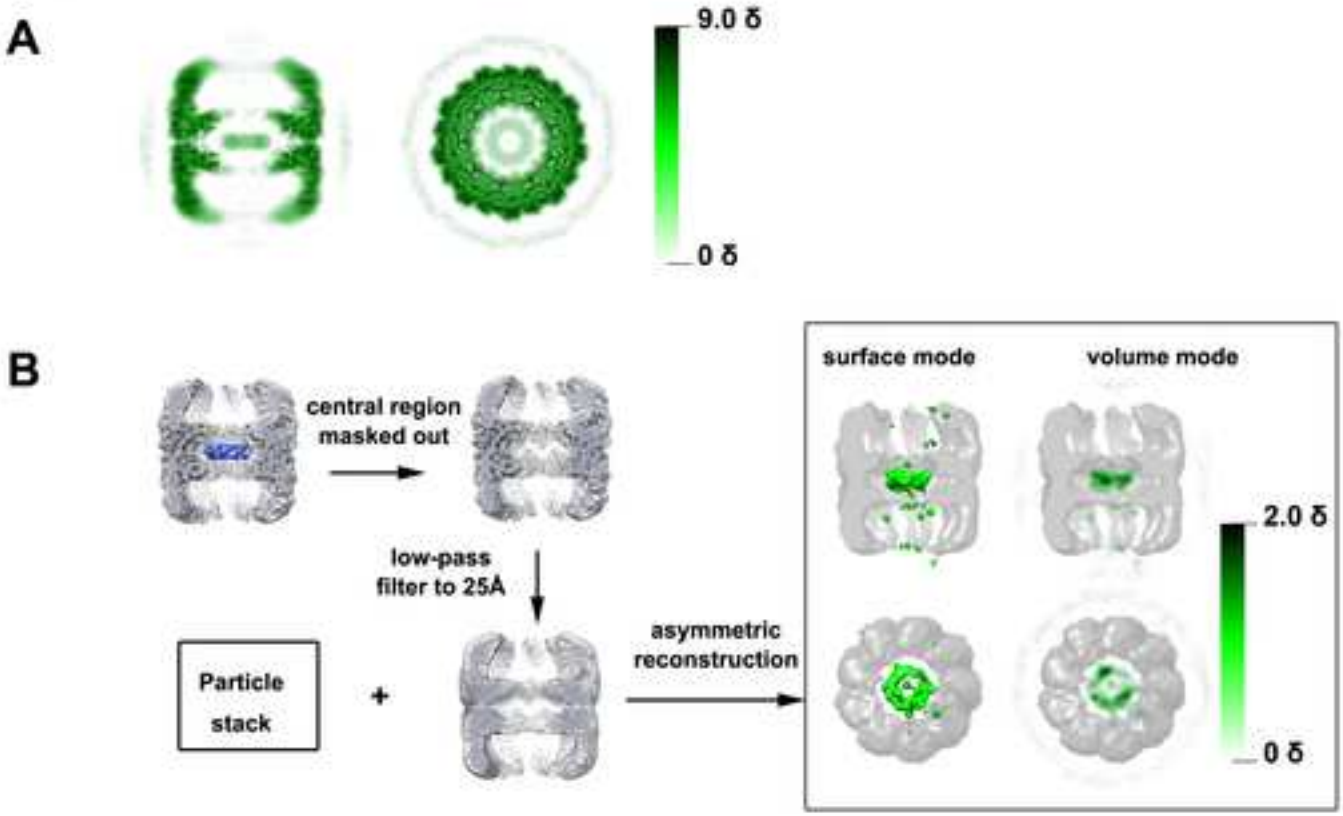

Figure S6
Click here to download high resolution image

Figure S6

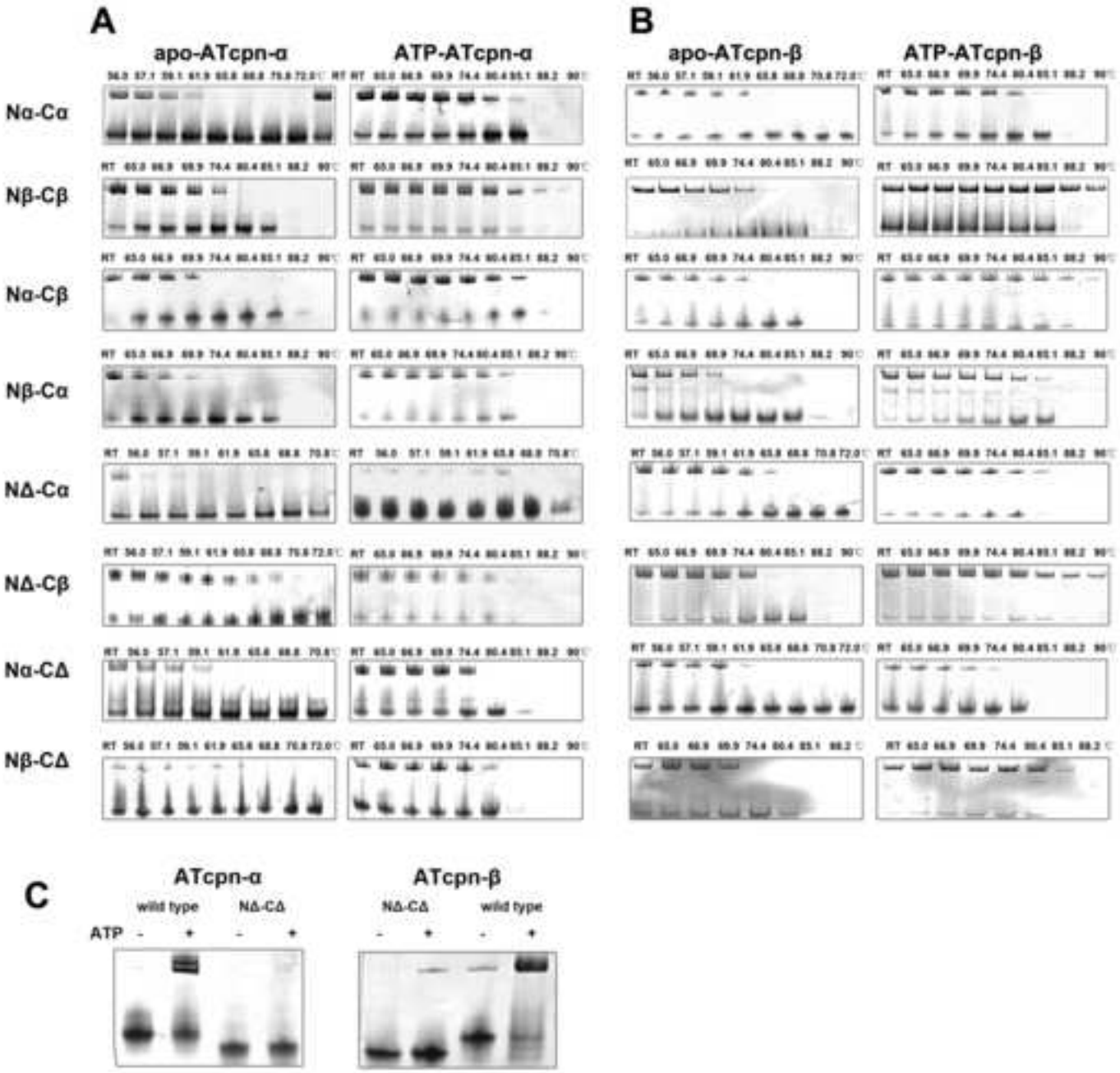

Figure S7
Click here to download high resolution image

Figure S7

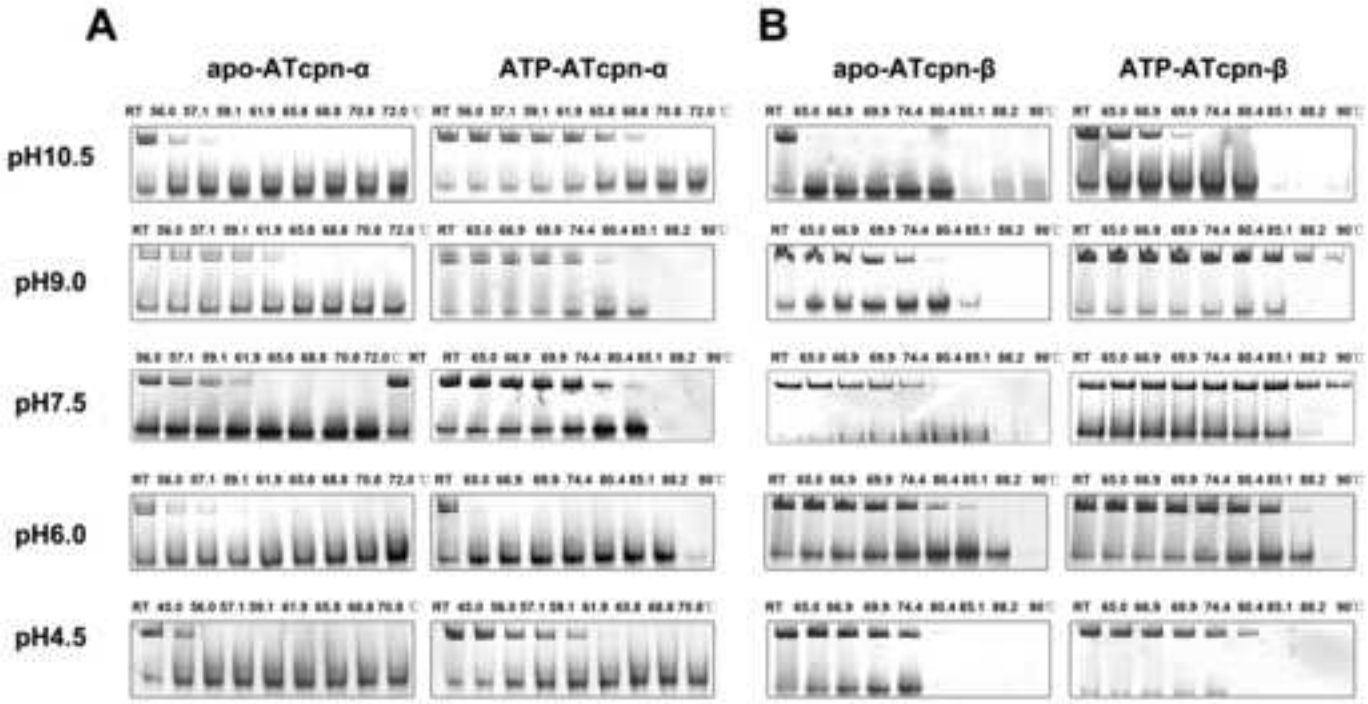

Supplemental Figure and Movie Legends

Figure S1. Time course experiments on the thermal stability of apo AT cpn-α by native PAGE (related to Figure 2B). The samples were heated, respectively, to (**A**) 45°C, (**B**) 50°C, (**C**) 55°C and (**D**) 60°C for 10 to 90 min before assayed by native PAGE. The lower bands represent monomers and the upper bands represent assemblies.

Figure S2. ATP hydrolysis is not relevant to the thermal stabilities of AT thermosomes (related to Figure 3). (**A, B**) Thermal stability experiments on D400A mutants of cpn-α and cpn-β in absence (left) or presence (right) of ATP by native PAGE. (**C**) Thermal stability experiments on cpn-α (left) and cpn-β (right) with the existence of ADP.

Figure S3. CryoEM reconstruction of AT cpn-α (related to Figure 4). (**A**) Raw cryoEM micrograph of apo cpn-α (left) and profile of its power spectrum (right). The inset shows that the information limit is higher than 4.0 Å. (**B**) 2D classification of apo cpn-α. Endview particles with 8-fold symmetry are highlighted by the green rectangle and particles with 9-fold symmetry by the red rectangle. (**C**) Projection-matching diagrams for the reconstructions of apo cpn-α with 8- and 9-fold symmetries. (**D**) Structural comparison between 8-fold (magenta) and 9-fold (red) apo AT cpn-α. Superposition between the subunits from 8- and 9-fold cpn-α indicates their high similarity (left). Their packing modes within one ring are compared from top views (right) and the green arrow indicates the twisting angle between their subunits.

Figure S4. The role of the lid domain in the thermal stability of AT cpn-α and cpn-β (related to Figure 4). (**A**) Thermal stability assays on the AT lidless cpn-α in the apo (left) and ATP-binding states (right). (**B**) Thermal stability assays on the AT lidless cpn-β in the apo (left) and ATP-binding states (right).

Figure S5. Validation and reliability of the central density of AT cpn-β (related to Figure 5). (**A**) Volume rendering of cpn-β in the ATP-binding state (the cryoEM map was filtered to 8.0 Å with a low-pass filter). (**B**) Asymmetric reconstruction of cpn-β in the ATP-binding state by using the low-pass filtered initial model with the central region

density masked out.

Figure S6. The role of the N/C-termini for the thermal stability of AT thermosomes (related to Figure 6A-E). (A) Thermal stability assays of all the N/C-termini variants of AT cpn-α in the apo (left) and ATP-binding states (right). **(B)** Thermal stability assays of all the N/C-termini variants of AT cpn-β in the apo (left) and ATP-binding states (right). **(C)** The assembly of wild types and N/C-termini deletion mutants of AT cpn-α (left) and cpn-β (right) with (**+**) and without (**-**).

Figure S7. Thermo stability assay of AT cpn-α and cpn-β in different pH values (related to Figure 6F). (A) Thermal stability assays on AT cpn-α in the apo (left) and ATP-binding states (right) in pH10.5, 9.0, 7.5, 6.0 and 4.5. **(B)** Thermal stability assays on AT cpn-β in the apo (left) and ATP-binding states (right) in pH10.5, 9.0, 7.5, 6.0 and 4.5.

Movie S1. Volume rendering of AT cpn-β in the ATP-binding state. The cryoEM map was filtered to 8.0 Å with a low-pass filter**.**

Movie S2. Surface and volume rendering of AT cpn-β in the ATP-binding state from the asymmetric reconstruction.

Table S1. Statistics of the cryoEM reconstructions and data entries

Sample name	MAG[1]	Binning	Pixel size	Number of particles used	Resolution (Å) at FSC[2]=0.5	Resolution (Å) at FSC[2]=0.143	EMDB[3] code (EMD-)	PDB[4] code
AT apo cpn-α (8 fold)	96000	1	0.933	55460	4.9	4.1	5391	3J1B
AT apo cpn-α (9 fold)	96000	2	1.866	9596	9.1	7.5	5392	3J1C
AT apo cpn-β (9 fold)	96000	2	1.866	23285	8.3	6.7	5395	3J1E
AT ATP-cpn-β (9 fold)	96000	2	1.866	28374	6.2	5.0	5396	3J1F

1. MAG, nominal magnification.

2. FSC, Fourier shell correlation coefficient.

3. EMDB, electron microscopy data bank.

4. PDB, protein data bank.

Table S2. Summary of the N- and C-termini deletion and swapping variations of AT cpn-α and cpn-β.

Sample name	Explanation
cpn-α-NΔCΔ	Main body of cpn-α, N- and C-termini deletion
cpn-α-NΔCα	Main body of cpn-α, N-termini deletion, C-termini from cpn-α
cpn-α-NΔCβ	Main body of cpn-α, N-termini deletion, C-termini from cpn-β
cpn-α-NαCΔ	Main body of cpn-α, N-termini from cpn-α, C-termini deletion
cpn-α-NαCα	cpn-α itself
cpn-α-NαCβ	Main body of cpn-α, N-termini from cpn-α, C-termini are from cpn-β
cpn-α-NβCΔ	Main body of cpn-α, N-termini from cpn-β, C-termini deletion
cpn-α-NβCα	Main body of cpn-α, N-termini from cpn-β, C-termini from cpn-α
cpn-α-NβCβ	Main body of cpn-α, N- and C-termini both from cpn-β
cpn-β-NΔCΔ	Main body of cpn-β, N- and C-termini deletion
cpn-β-NΔCα	Main body of cpn-β, N-termini deletion, C-termini from cpn-α
cpn-β-NΔCβ	Main body of cpn-β, N-termini deletion, C-termini from cpn-β
cpn-β-NαCΔ	Main body of cpn-β, N-termini from cpn-α, C-termini deletion
cpn-β-NαCα	Main body of cpn-β, N- and C-termini both from cpn-α
cpn-β-NαCβ	Main body of cpn-β, N-termini from cpn-α, C-termini are from cpn-β
cpn-β-NβCΔ	Main body of cpn-β, N-termini from cpn-β, C-termini deletion
cpn-β-NβCα	Main body of cpn-β, N-termini from cpn-β, C-termini from cpn-α
cpn-β-NβCβ	cpn-β itself

Δ: N- or C-terminus deletion

Nα: N-terminus of cpn-α, from M1 to S18

Cα: C-terminus of cpn-α, from S533 to S563

Nβ: N-terminus of cpn-β, from M1 to Y27

Cβ: C-terminus of cpn-β, from G533 to D553